Supporting Information for "Inner-layer Capacitance of Organic Electrolytes from Constant Voltage Molecular Dynamics"

Yi-Jung Tu, Samuel Delmerico, and Jesse G. McDaniel*

School of Chemistry and Biochemistry, Georgia Institute of Technology, Atlanta, Georgia 30332-0400

E-mail: mcdaniel@gatech.edu

1 Voltage-Dependent Density Profiles of Electrolyte Functional Groups

In Figures S1 , S2 , and S3, we show density distribution plots of the functional groups of acetonitrile, dichloroethane, and acetone solvent molecules near the electrode interfaces at different applied voltages. The analysis shown in Figures S1 , S2 , and S3 respectively correspond to the charge density analysis of the solvents shown in Figure 5, 6, and 7 of the main manuscript. The conclusions from the functional group density distribution analysis are similar to those discussed for the charge density analysis, namely the interfacial structure of acetonitrile and dichloroethane does not change much with applied voltage, but the interfacial structure of acetone exhibits significant rearrangement at higher applied voltage. The voltage-modulated rearrangement of acetone is apparent in Figure S3, as the density peaks for the –C=O dipole near the cathode/anode exhibit marked change with voltage.

The arrangements of interfacial solvent dipoles at high voltage can be observed in Figure S4. Near the anode, solvent dipoles for all three solvents are oriented normal to the surface. Near the cathode, interfacial acetonitrile and dichloroethane molecules remain parallel orientations with the surface at high voltage, whereas the –C=O dipole near the cathode is tilted with respect to the cathode surface.

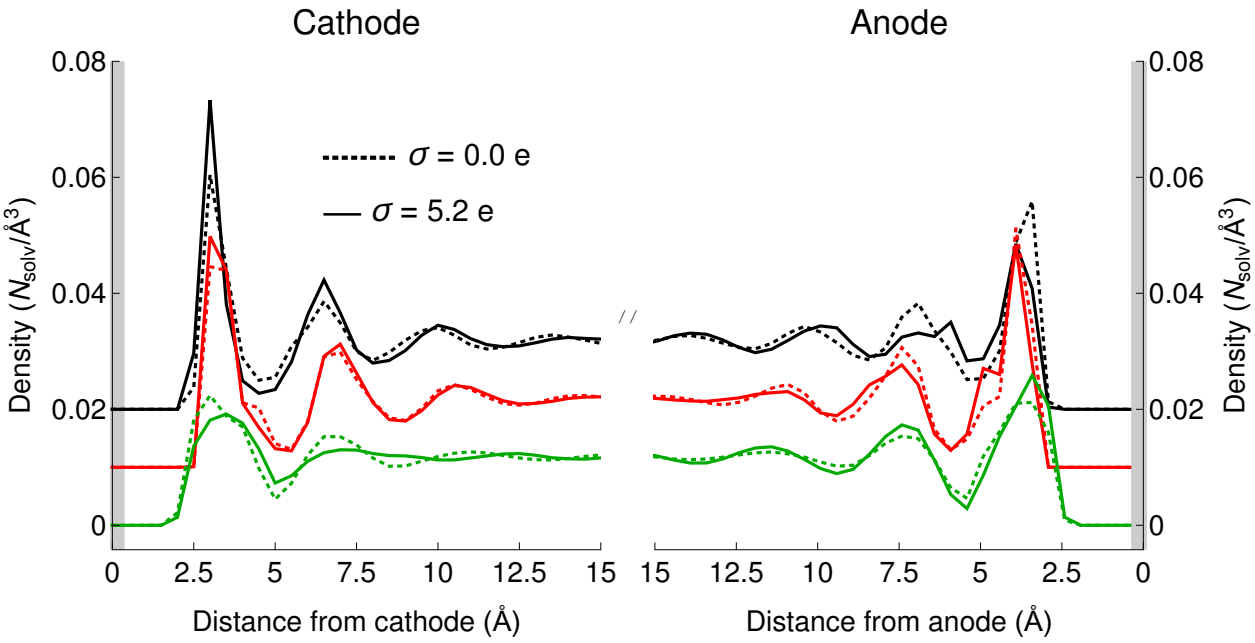

Figure S1: The density distribution profiles of –C≡N (the N atom in black color and the C atom in red color) and $-CH_3$ (green curves) groups for 1500 acetonitrile molecules as a function of total surface charges of 0 and 5.2 e, which correspond to applied voltage to cathode/anode at 0/0 and 1.1/–1.1 V.

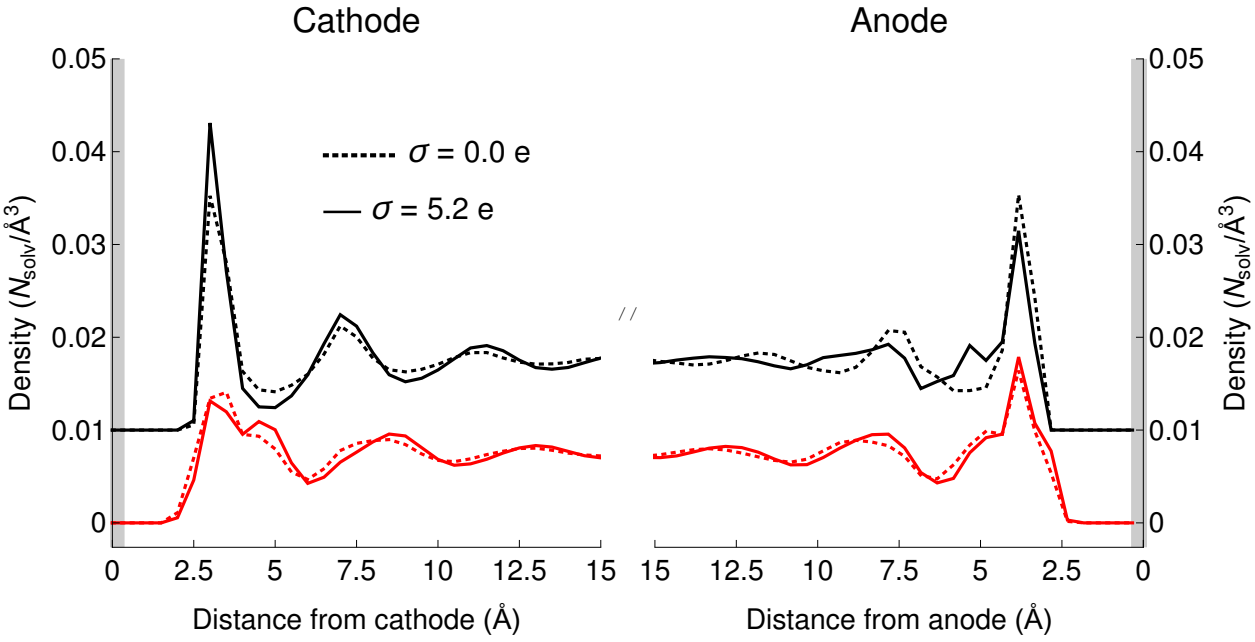

Figure S2: The density distribution profiles of –Cl (black curves) and $-CH_2CH_2$ (red curves) groups for 1500 dichloroethane molecules as a function of total surface charges of 0 and 5.2 e, which correspond to applied voltage to cathode/anode at 0/0 and 2/–2 V.

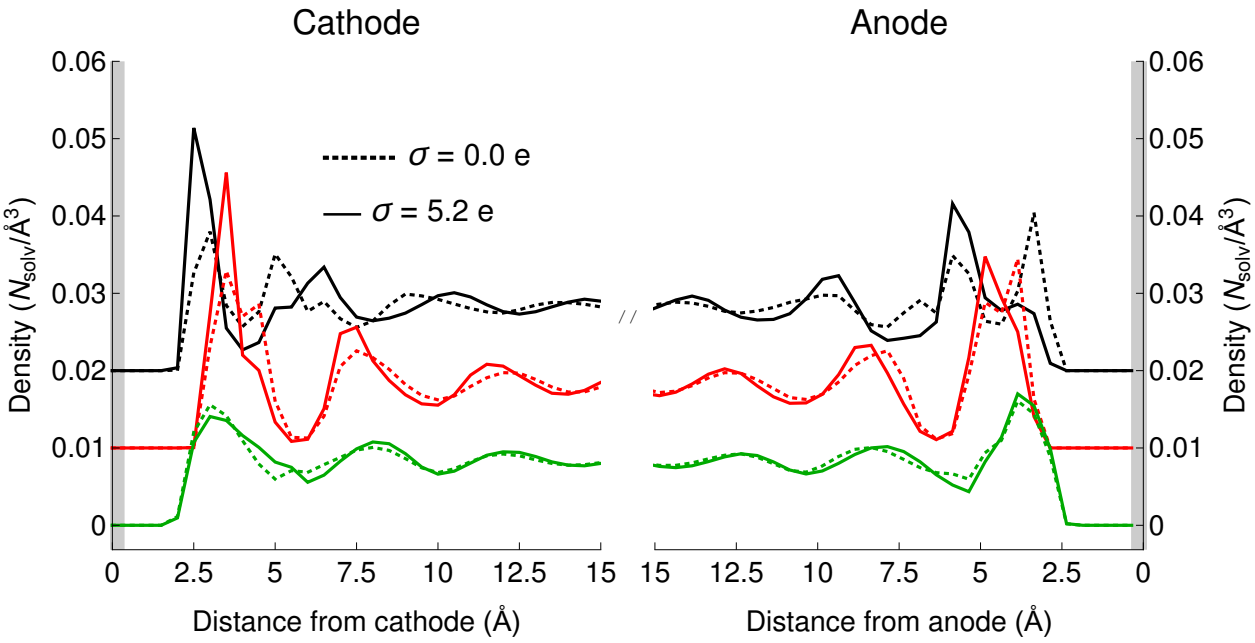

Figure S3: The density distributions of the –C=O (the O atom in black curves and the C atom in red curves), and –CH_3 (green curves) groups for 1500 acetone molecules as a function of total surface charges of 0 and 5.2 e, which correspond to applied voltage to cathode/anode at 0/0 and 1.5/–1.5 V.

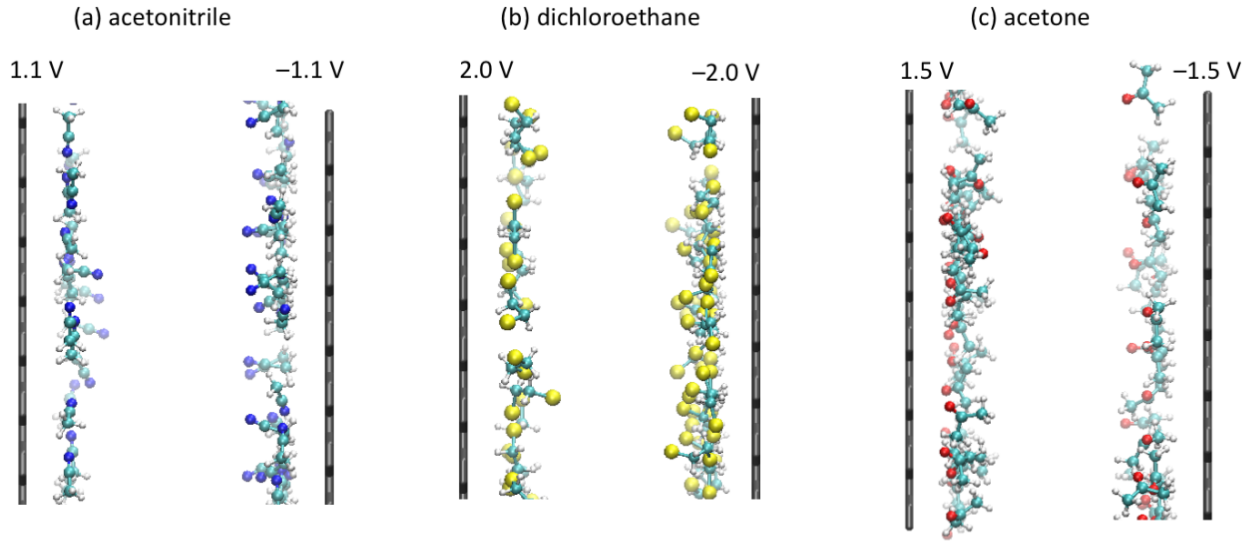

Figure S4: A randomly selected snapshot for the first layer (a) acetonitrile, (b) dichloroethane, and (c) acetone near the cathode and anode with total surface charge of 5.2 e.

For 10 mol% [$BMIm^+$][BF_4^-] /acetonitrile solution, density distribution plots of the functional groups of $BMIm^+$, and BF_4^-, and acetonitrile are shown in Figure S5, and the z-direction of dipole moment of the interfacial acetonitrile molecules is presented in Figure S6. In Figure S7, the Poisson potential of 10 mol% [$BMIm^+$][BF_4^-] /acetonitrile solution shows that the voltage drop near the cathode is smaller than anode at low and high applied voltages. Because the surface charge on cathode and anode are equal in magnitude, the larger voltage drop near the anode corresponds to the smaller capacitance, which indicates that the total capacitance is limited by the capacitance at anode. Similar to 10 mol% [$BMIm^+$][BF_4^-] /acetonitrile solution, the Poisson potential for neat [$BMIm^+$][BF_4^-] also shows the total capacitance is anode limited (Figure S8).

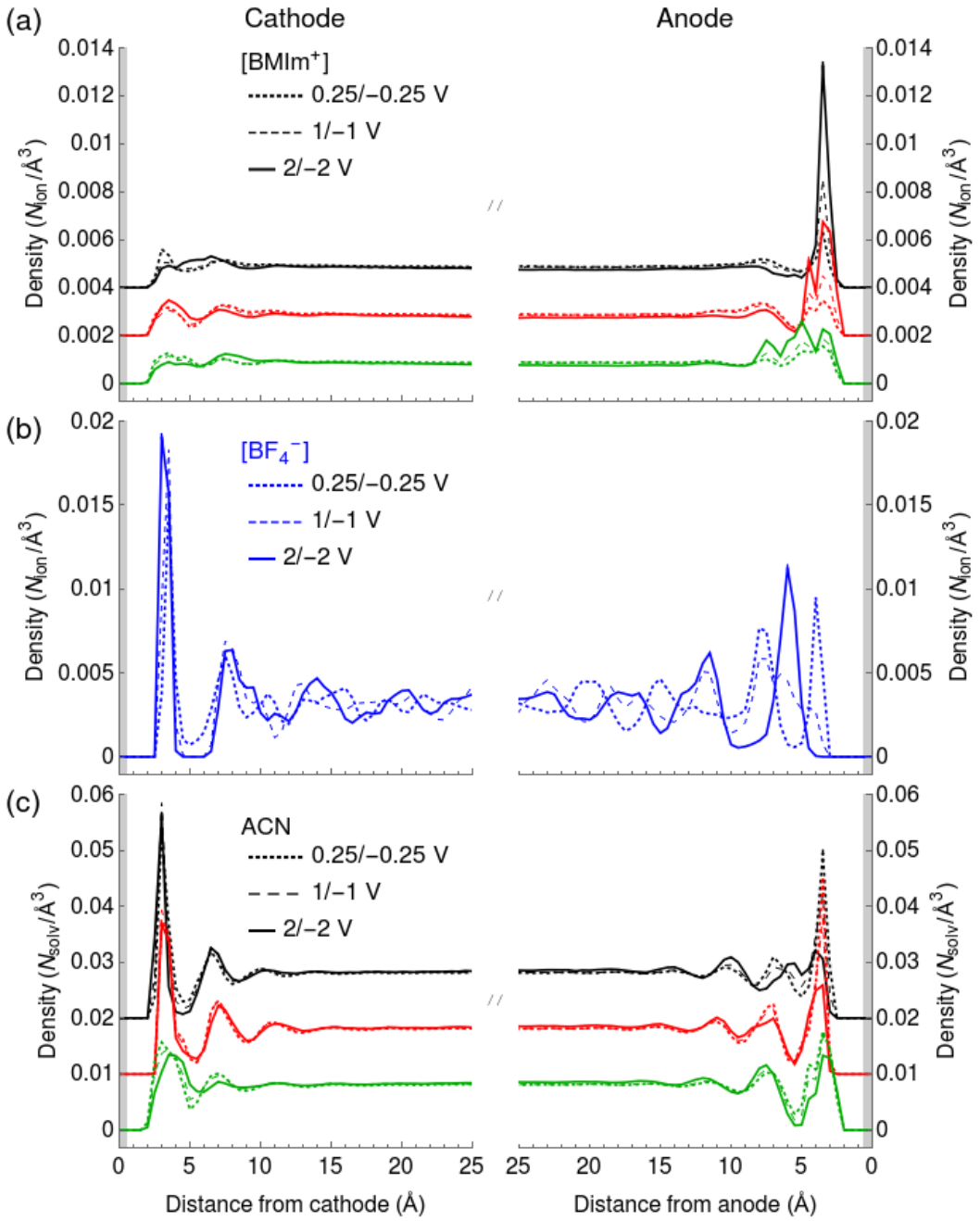

Figure S5: Density profiles for 10 mol% [$BMIm^+$][BF_4^-] /acetonitrile solution for (a) the –Im (black curves), $–CH_3$ (red curves), and $–C_4H_9$ (green curves) groups of $BMIm^+$, (b) BF_4^-, and (c) the –C≡N (the N atom in black color and the C atom in red color) and $–CH_3$ (green curves) groups of acetonitrile molecules when the applied voltage to cathode/anode are at 0.25/–0.25, 1/–1, and 2/–2 V.

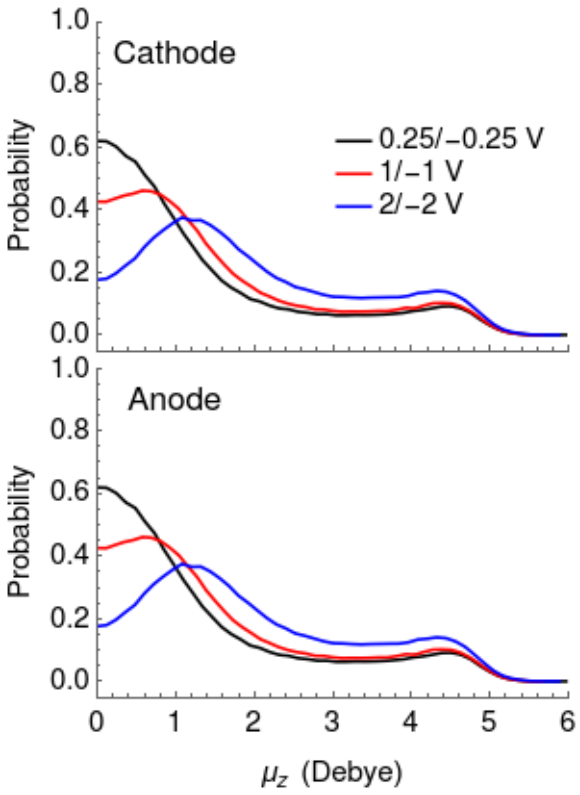

Figure S6: Dipole moment distributions of interfacial acetonitrile molecules for 10 mol% [BMIm$^+$][BF$_4^-$] /acetonitrile solution when the applied voltage to cathode/anode (V$_{cathode}$/V$_{anode}$) are at 0.25/–0.25, 1/–1, and 2/–2 V.

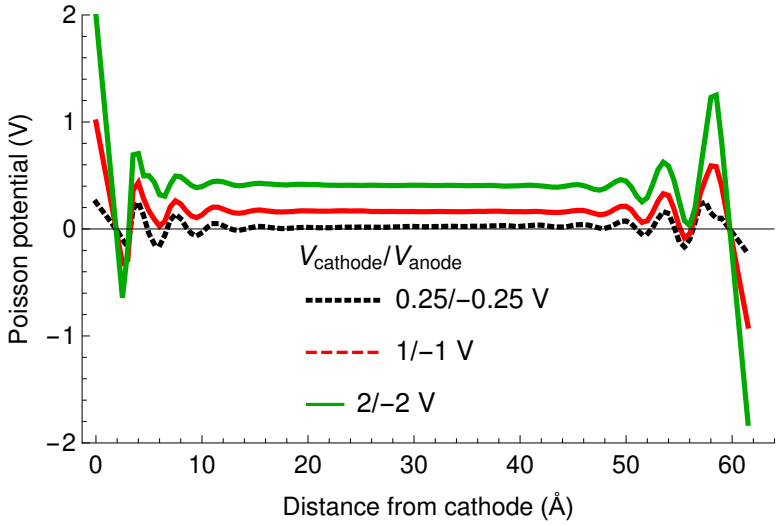

Figure S7: Poisson potential of the charge distribution for 10 mol% [BMIm$^+$][BF$_4^-$] /acetonitrile solution when the applied voltage to cathode/anode (V$_{cathode}$/V$_{anode}$) are at 0.25/–0.25, 1/–1, and 2/–2 V.

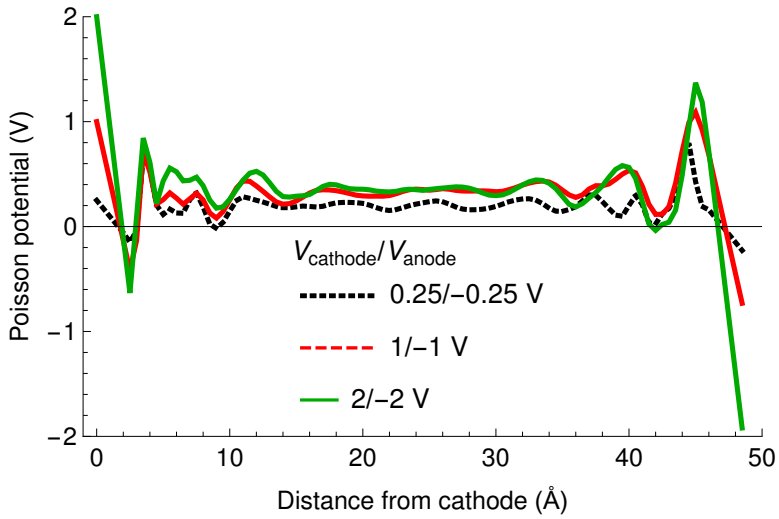

Figure S8: Poisson potential of the charge distribution for 300 ion pairs of $[BMIm^+][BF_4^-]$ when the applied voltage to cathode/anode ($V_{cathode}/V_{anode}$) are at 0.25/–0.25, 1/–1, and 2/–2 V.

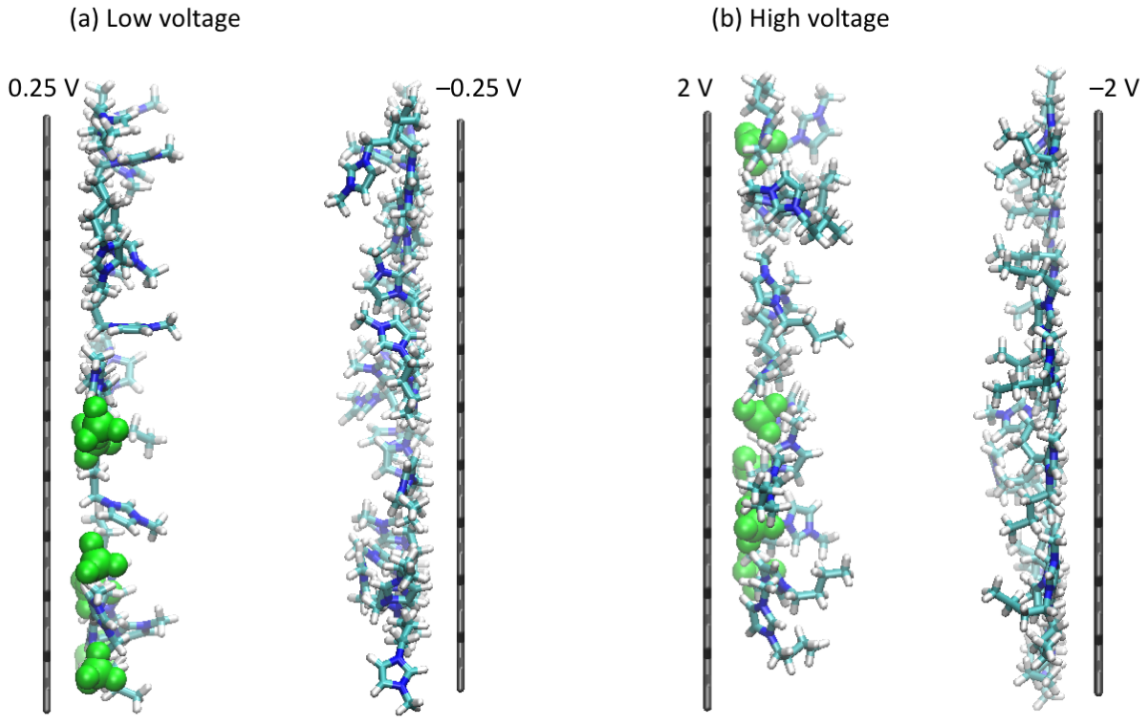

Figure S9: MD snapshots for interfacial $[BMIm^+][BF_4^-]$ near the cathode and anode at (a) low and (b) high applied voltages.

2 Benchmark of Monte Carlo Approach for NPT Density Equilibration

We describe and benchmark our Monte Carlo (MC) approach for equilibrating the electrolyte density between two "frozen" and perfectly flat graphene sheets which serve as the electrodes in our system; we refer to this as our MC-NPT procedure. After equilibration with the MC-NPT simulations, we run constant voltage MD simulations to compute capacitance of the systems; benchmarks for our fixed voltage algorithm are given in Section 3.

As a benchmark for our MC-NPT procedure, we employ an electrolyte composed of 100 $[BMIm^+][BF_4^-]$ ion pairs and 1000 acetonitrile solvent molecules, sandwiched between two graphene electrodes. The graphene sheets are infinitely periodic in the X/Y plane, with 800 carbon atoms (per graphene sheet) in the principle simulation box, giving rise to box vectors of 4.93 nm in length, at a 120^o angle for the basal graphene plane. We label the Z dimension as being perpendicular to the basal graphene (electrode) plane.

Our constant potential method is designed for "perfectly flat" electrodes (Section 3). Therefore, we cannot simply run a simulation propagating the Newtonian equations of motion for the graphene carbon atoms, which would lead to deformation of the flat graphene sheets (with the extent of deformation depending on the bond, angle, torsion terms of the force field). We thus employ a hybrid molecular dynamics/Monte Carlo (MD/MC) approach to enforce that the graphene sheets stay flat while equilibrating the electrolyte density at constant pressure. During the MD steps, the positions of the electrodes are frozen and are not propagated (MD propagates the atoms of the electrolyte only), and Monte Carlo (MC) moves are used to move the positions of the graphene sheets, and thus equilibrate the electrolyte density.

The MC moves satisfy detailed-balance conditions within the isothermal-isobaric (NPT) ensemble at 300 K and 1 bar. Each MC step consists of randomly moving the graphene sheet in the +/- Z direction (we only move one electrode sheet for simplicity), and scaling

the electrolyte molecules center-of-mass (COM) positions, as is typical in an NPT volume move. The graphene sheet is given a random displacement between -0.5 Å and 0.5 Å along the Z dimension, while the other sheet (electrode) is fixed. This trial displacement of the sheet changes the accessible volume of the electrolyte from V to V' = V + ΔV, where (ΔV) is determined by the change of distance between two electrode plates, given the constant surface area (XY dimensions) of the electrode.

After the graphene sheet is randomly moved, there is a new separation distance between electrodes along the z dimension; call this separation distance the 'new box length'. The COM positions of all electrolyte molecules are then scaled according to the ratio of the new and old box lengths. Note that we only scale the COM positions, and not the positions of all atoms so that the bonds and angles of the molecules are not distorted in an energetically unfavorable way (which would lead to low acceptance probablities and/or detailed balance issues). The potential energy (E') of this new configuration (with shifted graphene sheet, COM electrolyte positions) is calculated. To derive the detailed balance condition, it is standard to do a coordinate transformation (see Frenkel, Smit, "Understanding Molecular Simulation: From Algorithms to Applications") to fractional COM coordinates, and internal coordinates, and the probability for these volume moves then only applies to N_{Mol} COM degrees of freedom (N_{Mol} is the total number of all molecules). Applying the Metropolis algorithm to the detailed balance condition gives the following probability for accepting volume moves:

$$acc_{old->new} = 1 \text{ if } \omega \leq 0$$

$$acc_{old->new} = exp\left(-\omega\beta\right) \text{ if } \omega > 0$$

where ω = (E'–E) + P(V'–V) + N_{Mol} β^{-1} ln(V'/V), $\beta = 1/(k_b{*}T{*}N_A)$, k_b is the Boltz-

mann constant, P is 1 bar, T is at 300 K, and N_A is the Avogadro constant. The maximum displacement for the graphene sheet move is dynamically adjusted such that the acceptance ratio of the moves falls between 25–75 % (this is a somewhat arbitrary choice, but is in line with the commonly targeted $\sim$ 40% acceptance goal). We perform 25 steps of MD integration for each MC move. We choose a friction coefficient of 1 ps^{-1} for the Langevin temperature thermostat, which we find is sufficient for thermal equilibration after volume moves.

As a benchmark for our NPT Monte Carlo approach, in Figure S10 we compare the density profile of acetonitrile solvent (ACN) computed from a bulk NPT simulation and computed from a system of solvent confined between two graphene electrodes, equilibrated by NPT Monte Carlo. We do this comparison for two different system sizes, with systems of 1000 ACN and 2000 ACN for both the bulk, and confinement simulations. The density profiles for both 1000 and 2000 acetonitrile molecules in the confined system yield the density of 0.0118 $N_{ACN}/\mathring{A}^3$ (0.80 g/cm^3) within the middle of the simulation cell, which is within 1 % of the reference bulk systems (0.0117 $N_{ACN}/\mathring{A}^3$ = 0.80 g/cm^3). This indicates that the density profiles for the confined systems are in good agreement with those for the bulk, for various system sizes.

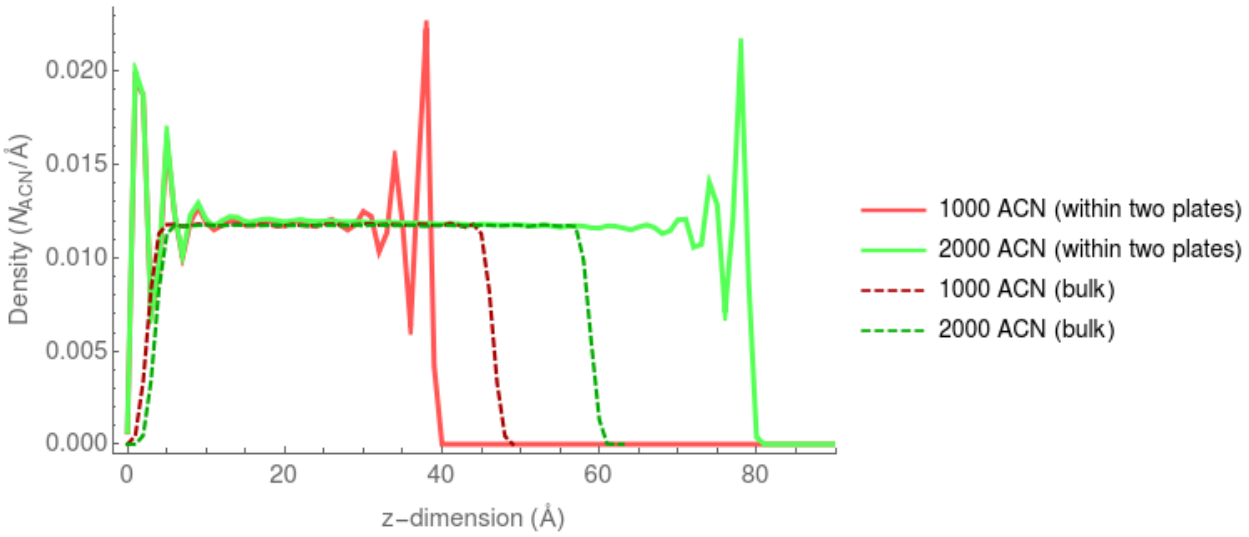

Figure S10: The density profiles of 1000 (red) and 2000 (green) acetonitrile molecules in the confined system (solid line) and the corresponding bulk system (dashed line).

In this study, simulations were performed with organic solvents, $[BMIm^+][BF_4^-]$ solutions in acetonitrile, and neat $[BMIm^+][BF_4^-]$. The lengths of these simulation cells obtained from NPT density equilibration are summarized in Tables S1, S2, and S3.

Table S1: The system sizes of solvents and the corresponding cell lengths

Solvents	number of molecules	L_{cell} (nm)	L_{vac}[a](nm)	C_{vac}[b](μF/cm^2)
acetonitrile	1000	4.32	7.73	6.04×10^{-4}
	1500	6.34		
	2000	8.35		
acetone	1000	6.04		
	1500	8.89		
	2000	11.70		
1,2-dichloroethane	1000	6.63		
	1500	9.83		
	2000	12.93		
chloroform	1000	6.63		
	1500	10.01		
	2000	13.09		

[a] the distance across the vacuum after MC equilibration.
[b] $C_{vac} = \epsilon_0 A/L_{vac}$, where A is area of a graphene sheet

Table S2: The system sizes and cell lengths as a function of the $[BMIm^+][BF_4^-]$ content (mol%) in acetonitrile

$[BMIm^+][BF_4^-]$ contents	number of ion pairs/solvent molecules	L_{cell} (nm)
1	15 / 1500	6.64
2	30 / 1500	6.80
5	55 / 1000	5.13
10	110 / 1000	6.17
18	220 / 1000	7.57
37	300 / 500	6.84
50	300 / 300	6.08
75	300 / 100	5.27
100	400 / 0	6.40

Table S3: The system sizes for 1 and 2 mol% of [BMIm$^+$][BF$_4^-$] /acetonitrile mixtures and neat [BMIm$^+$][BF$_4^-$]

[BMIm$^+$][BF$_4^-$] content	number of molecules	L_{cell} (nm)	L_{vac}[a](nm)	C_{vac}[b](μF/cm^2)
1 mol%	10 / 1000	4.47		
	15 / 1500	6.64		
	20 / 2000	8.65		
2 mol%	20 / 1000	4.62		
	30 / 1500	6.80		
	40 / 2000	8.96		
neat [BMIm$^+$][BF$_4^-$]	300	4.86	15.18	6.04×10^{-4}
	400	6.40		
	500	7.92		

[a] the distance across the vacuum after MC equilibration.
[b] $C_{vac} = \epsilon_0 A/L_{vac}$, where A is area of a graphene sheet

3 Benchmark of Constant Voltage Method

In the main manuscript, we have described our method for fixing the Voltage difference between two electrodes, and optimizing the charges on the electrode surface. Here, we benchmark our choice of settings/parameters that we utilize in this approach.

For modeling the electrodes at constant voltage, our theoretical algorithm involves computing the electric field at discrete points on the electrode, and subsequently solving for the surface charges. The external potential specifies the boundary condition of the electric field at the electrode, corresponding to the voltage drop over the vacuum gap. Surface charges are derived by dividing the surface of each electrode into discrete Gaussian pillboxs, and solving Gauss's law satisfying the fixed voltage boundary condition. As discussed in Section 2, the electrodes (graphene sheets) are kept perfectly flat so that the electric flux across each pillbox is entirely from the z-component.

3.1 Frequency for optimizing the surface charges

The surface charges of the electrodes fluctuate as response to the rearrangements in the electrolyte near the electrode surface. To explicitly account for image charge fluctuations (and keep the Voltage fixed), the charges on electrodes must be recalculated throughout the simulations. An"adiabatic" treatment of electrode charge would involve re-optimizing charges at every MD time step, analogous to the treatment of electronic polarization (Drude oscillators) of electrolyte molecules. However, as we will show (and benchmark), it is generally a very good approximation to update electrode charges less frequently than every time step; i.e. the computed surface charges can be used for a number of simulation steps before they need to be recalculated. Appropriate choice of update frequency is important to minimize the cost by reducing the frequency of surface charge computation, without sacrificing accuracy.

To benchmark the appropriate frequency for electrode charge updates, We compute the correlation function, $\langle q_i(0)q_i(t)\rangle$ for the electrode charges. Figures S11–S13 show this correlation function at different voltages for a system consisting of [$BMIm^+$][BF_4^-] /ACN electrolyte, computed from simulations with electrode charge update frequency every 1, 10, or 50 timesteps (timesteps are 1 fs). For the range of applied voltages (0-4V), we find that the surface charge correlation functions are very similar for charge updates of 1, 10, and 50 steps. For update frequencies of every step (1 fs), the correlation time for charge relaxation on cathode/anode are 0.7/0.75, 0.75/0.6, 0.6/0.55 ps at 1, 2, and 4 V. respectively. Similar relaxation times computed from 10 and 50 fs charge update frequency are listed in Table S4. This comparison, and the fact that the charge correlation function has a significantly longer correlation time than the update frequency, indicates that either 1, 10, or 50 fs update frequency should provide equally good accuracy, and we choose 50 fs update frequency for enhanced computational efficiency.

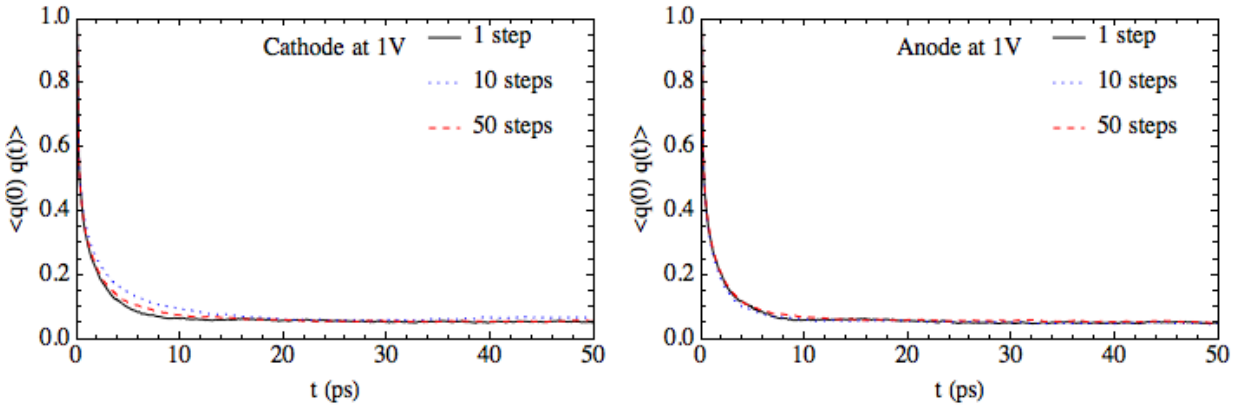

Figure S11: The autocorrelation function of surface charges over time, with charges computed every 10 and 50 steps, when a mixture of 100 [BMIm$^+$][BF$_4^-$] and 1000 ACN is simulated at 1V.

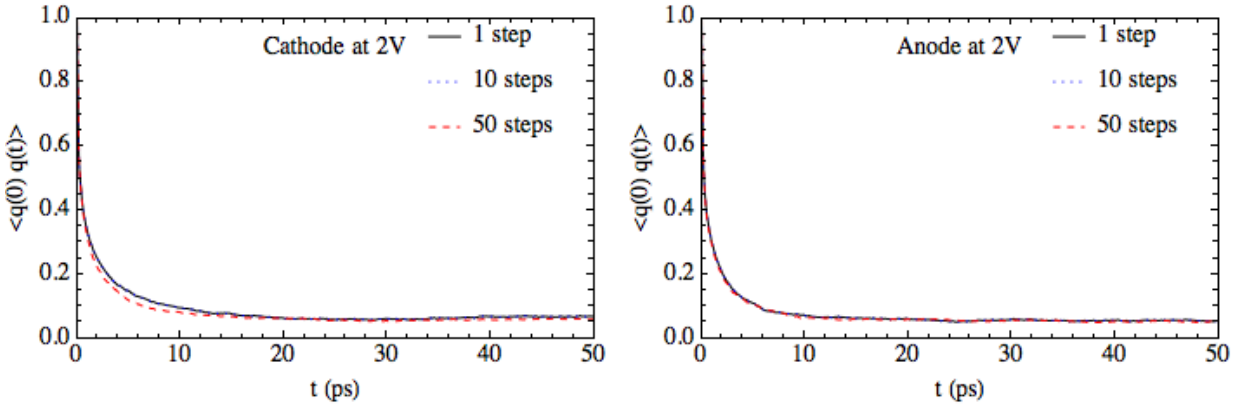

Figure S12: The autocorrelation function of surface charges over time, with charges computed every 10 and 50 steps, when a mixture of 100 [BMIm$^+$][BF$_4^-$] and 1000 ACN is simulated at 2V.

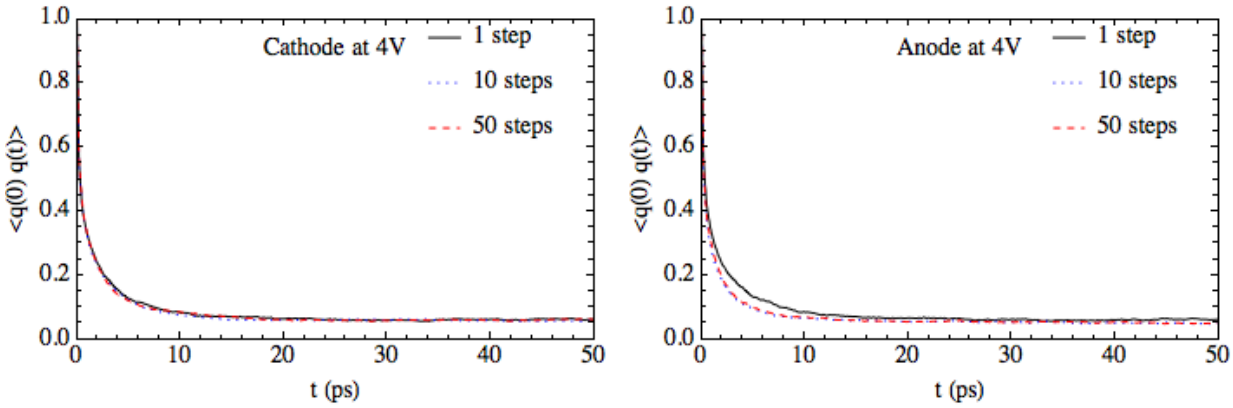

Figure S13: The autocorrelation function of surface charges over time, with charges computed every 10 and 50 steps, when a mixture of 100 [$BMIm^+$][BF_4^-] and 1000 ACN is simulated at 4V.

Table S4: Comparison of charge relaxation time for computing charges every 1, 10, and 50 steps

		Cathode (ps)	Anode (ps)
Solution	$\Delta V_{applied}$	1/ 10 / 50 steps	1 / 10 / 50 steps
100 [$BMIm^+$][BF_4^-] /1000 ACN	1 V	0.60 / 0.75 / 0.65	0.55 / 0.55 / 0.65
100 [$BMIm^+$][BF_4^-] /1000 ACN	2 V	0.75 / 0.75 / 0.70	0.60 / 0.60 / 0.55
100 [$BMIm^+$][BF_4^-] /1000 ACN	4 V	0.70 / 0.70 / 0.75	0.75 / 0.50 / 0.55

To further benchmark the choice of charge update frequency (every 10 or 50 steps), we compute dynamics properties of the [$BMIm^+$][BF_4^-] /ACN electrolyte, namely the ion diffusion coefficients and ion residence time on the electrodes. **We note that the benchmarks shown in Table S5 and Table S6 should only be interpreted qualitatively, as they were computed from relatively short $\sim$ 5 ns simulations. 5 ns is an order of magnitude shorter than simulation times necessary for converged predictions of ionic liquid dynamics, and thus the results should only be considered "semi-quantitative"**. The diffusion coefficients of the ions are given in Table S5 as computed from 10 and 50 step charge updates. In Table S6, we give the residence time of the ions near the electrodes as computed for the different charge update frequencies. Within statistical

uncertainty, these quantities are similar regardless of electrode charge update frequency: diffusion coefficients for the cations are 3.82×10^{-6} cm^2/s for 10 step updates and 3.95×10^{-6} cm^2/s for 50 step updates, and for the anions are 4.93×10^{-6} cm^2/s for 10 step updates and 4.68×10^{-6} cm^2/s for 50 step updates at 1V applied potential, indicating insignificant dependence on update frequency.

Table S5: Comparison between 10 and 50 time step of charge recalculation for diffusion coefficients (cm^2/s) of $BMIm^+$ (D_{BMIm}) and BF_4^- (D_{BF_4}) at various potential drops

Solution	$\Delta V_{applied}$	D_{BMIm} 10 steps / 50 steps	D_{BF_4} 10 steps / 50 steps
100 [$BMIm^+$][BF_4^-] /1000 ACN	1 V	3.82×10^{-6} /3.95×10^{-6}	4.93×10^{-6} / 4.68×10^{-6}
100 [$BMIm^+$][BF_4^-] /1000 ACN	2 V	4.48×10^{-6} / 3.98×10^{-6}	4.98×10^{-6} / 5.22×10^{-6}
100 [$BMIm^+$][BF_4^-] /1000 ACN	4 V	4.0×10^{-6} / 4.49×10^{-6}	4.25×10^{-6} / 5.00×10^{-6}

Similar to diffusion coefficients, the residence time of electrolyte ions is largely invarient to charge update frequency (within simulation uncertainty), as illustrated in Table S6. For 10 fs update frequency, the residence time of $BMIm^+$ at anode is 133, 142, and 179 ps at 1, 2, and 4V, respectively. For BF_4^-, the residence time on cathode is 175, 152, 266 ps at 1 V, 2V, and 4V (we see no physical reason for a shorter residence time at 2V compared to 1V, and believe this is just statistical uncertainty). For 50 fs update frequency, the residence times of $BMIm^+$ and BF_4^- ions are similar. It is important to note that the time for electrode charge relaxation is at least a hundred times shorter compared to that for ion structural relaxation, indicating that updating the electrode charges every 50 steps yields efficiency gains without compromising accuracy.

Table S6: Residence time of $BMIm^+$ (t_{BMIm}) and BF_4^- (t_{BF_4}) on the electrode as a function of the applied potential and the time steps to compute surface charges

Solution	Applied voltage	t_{BMIm} (ps) 10 steps / 50 steps	t_{BF_4} (ps) 10 steps / 50 steps
100 [$BMIm^+$][BF_4^-] /1000 ACN	1 V	133 / 158	175 / 166
100 [$BMIm^+$][BF_4^-] /1000 ACN	2 V	142 / 198	152 / 318
100 [$BMIm^+$][BF_4^-] /1000 ACN	4 V	179 / 289	266 / 338

3.2 Benchmark of Electric field in vacuum gap

We employ Neumann boundary conditions (e.g. specifying E_z) to solve Poisson's equation under the applied Voltage and periodic boundary conditions, which guarantees a unique solution. The unique solution for the electric field within the vacuum gap, is $E_z = \Delta V / L_{gap}$, where L_{gap} is the length of vacuum gap (between the two electrodes), and ΔV is the voltage drop between electrodes. We thus assess the accuracy of our numerical solution by benchmarking the magnitude of the electric field within the vacuum gap. To compute the electric field profile in the vacuum gap, we place a He atom as a probe in the vacuum gap and conduct a scan starting from 3.5 Å from the anode, to 3.5 Å to the cathode, in increments of 0.1 Å along the Z coordinate. For practical reasons, it is necessary to place a test charge on He; note this test charge slightly perturbs the system due to the corresponding electrode image charge(s); to minimize the perturbation on the system the charge on He should be sufficiently small and was set to be 0.001 a.u.

We benchmark the electric field within the vacuum gap for a system consisting of 100 [$BMIm^+$][BF_4^-] ion pairs and 1000 acetonitrile solvent molecules at applied potential of 2 V. These electric field benchmarks utilize randomly chosen snapshots of particular electrolyte configurations. The "final" method that we employ is described in Section 3.2.3, which utilizes both an analytic correction to numerically derived surface charges as well as "dummy" atoms paced in the middle of the honeycomb graphene lattice to improve discretization

resolution. Before describing this final method, we systematically benchmark increasing accuracy approximations, starting with the "zeroth-order" approach.

3.2.1 "zeroth-order" approach

The electric field components on the probe He atom are shown in Figure S14, plotted as a function of the He distance to the electrodes. The electric fields are around 0 V/L_{gap} for the X and Y components and around 2 V/L_{gap} for the Z component. However, the X, Y and Z components of electric fields are slightly shifted across the vacuum gap, with the shift in the Z component most obvious. These shifts indicate numerical error relative to the analytic solution of $|E_x|$=$|E_y|$=0 and $|E_z|$=2V/L_{gap}. Note that the numerical noise close to the electrodes is intrinsic due to the atomistic point charge representation of the electrode surface charge density. To remedy this numerical error, we investigate the placement of dummy atoms within the carbon atom lattice to increase discretization resolution of the electrode surface.

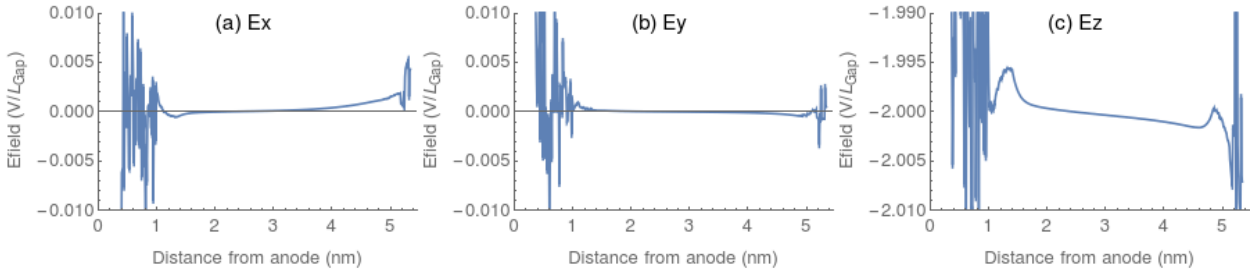

Figure S14: The electric field profiles in the vacuum gap (L_{Gap} = 6.24 nm) for "zeroth-order" algorithm, when the system was simulated at the applied potential of 2 V between two flat graphene sheets.

3.2.2 Dummy atoms on graphene sheets

We attempt to improve the accuracy of our numerical approach by adding "dummy atoms" to the graphene sheets to enhance the resolution of surface charge density, essentially reducing the size of the "Gaussian pillboxes" used for the numerical solution. These dummy atoms were placed in the middle of the carbon "honeycomb" lattices on the graphene sheets, and

the charge on the dummy atom is allowed to fluctuate. Analogous electric field analysis upon incorporation of these extra "dummy atoms" is shown in Figure S15. With the extra dummy atoms, the E_x and E_y field components are somewhat improved, but the systematic shift in the E_z component is still present.

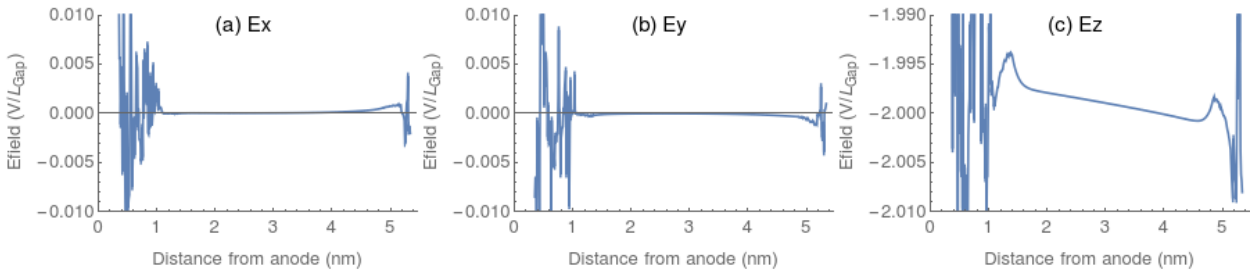

Figure S15: The electric field profiles in the vacuum gap (L_{Gap} = 6.24 nm) with inclusion of extra dummy atoms, when the system was simulated at the applied potential of 2 V between two flat graphene sheets.

3.2.3 Dummy atoms with analytical correction

Our final method involves employing an analytic correction to the derived surface charges, as described in the main manuscript. This analytic correction is derived using Green's reciprocity theorem, which gives an analytic formula for the total charge on the electrode as a function of the specific Voltage and configuration of the electrolyte. By calculating the analytic net charge, we can estimate the error in our numerical solution to the Poisson equation. We then determine final electrode atomic charges by scaling the numerical atomic charges by the ratio of total surface charge determined analytically and numerically. During each iteration of charge computation, the analytic solution is recomputed, and numerically derived charges are scaled accordingly. We benchmark the effect of this analytic charge scaling in Figure S16, which shows similar analysis of electric field components within the vacuum gap. With inclusion of extra graphene atoms and the charge scaling, the electric field profiles for x, y, and z components are constant, indicating the final approach with charge scaling provides an accurate method. We note that the "cusp" in the E_z field component close to the electrodes is due to the image charge interaction with the He "probe charge". The

He probe induces an "image charge" on the electrode, modulating the field. The field from the probe image charge falls as the inverse square distance of the probe from the electrode (as easily seen from image charge analysis), which results in the cusps in Figure S16. The comparisons of the numerical to analytic charges are shown in Figures S17 and S18.

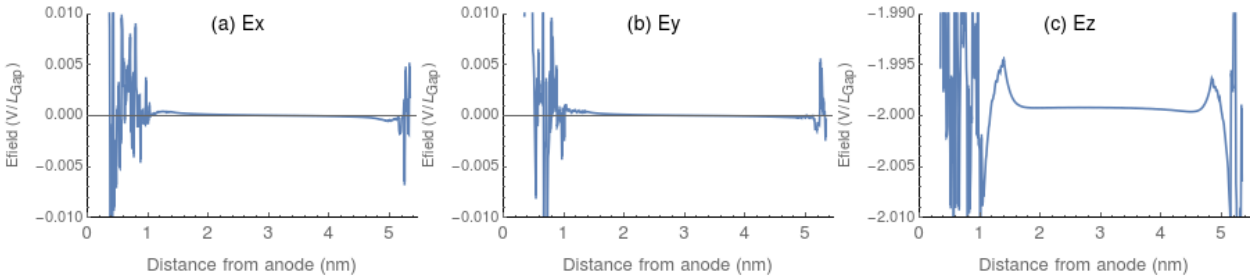

Figure S16: The electric field profiles in the vacuum gap with inclusion of extra dummy atoms and applied analytic correction, when the system was simulated at the applied potential of 2 V between two flat graphene sheets, where L_{Gap} = 6.24 nm.

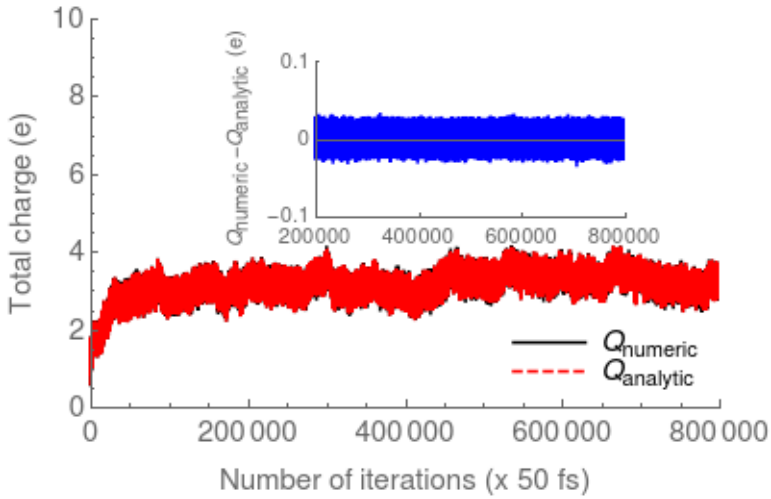

Figure S17: Comparison of the total charges computed numerically and analytically when the applied voltage to cathode/anode is at 0.5/–0.5 V. The inset shows the difference of the numerical and analytic charges.

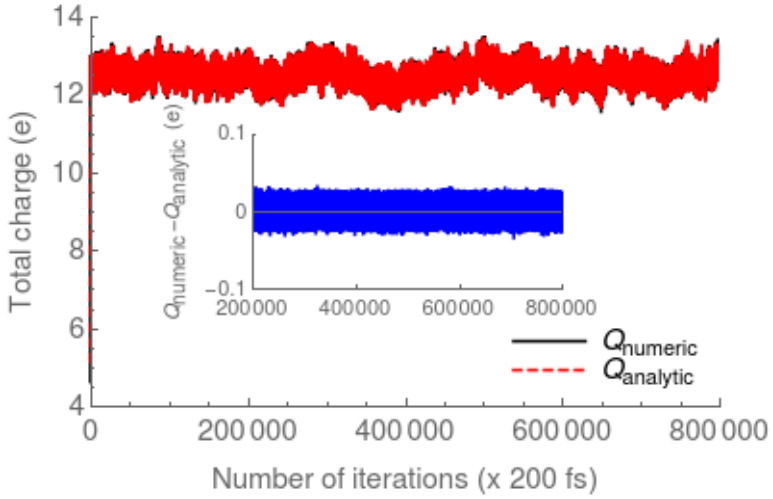

Figure S18: Comparison of the total charges computed numerically and analytically when the applied voltage to cathode/anode is at 2/–2 V. The inset shows the difference between the numerical and analytic charges.

4 The differential capacitances computed for 1/–1 V

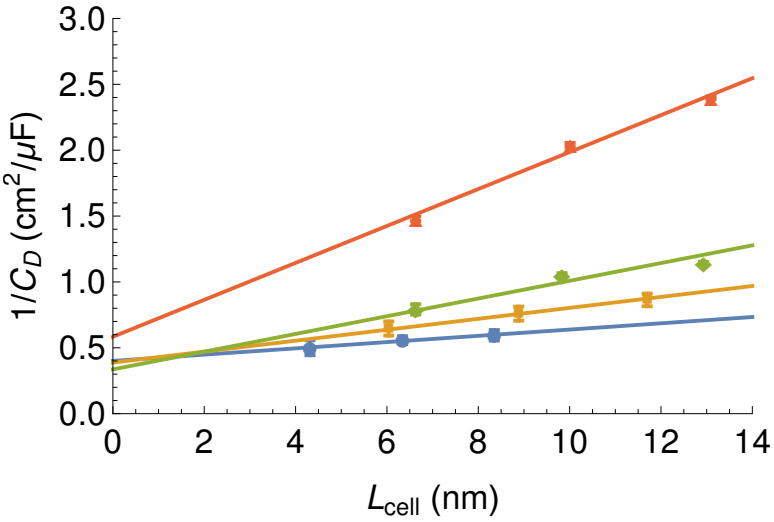

Figure S19: The inverse of total differential capacitance as a function of the cell lengths for the solvents when the applied voltage is at 1/–1 V.

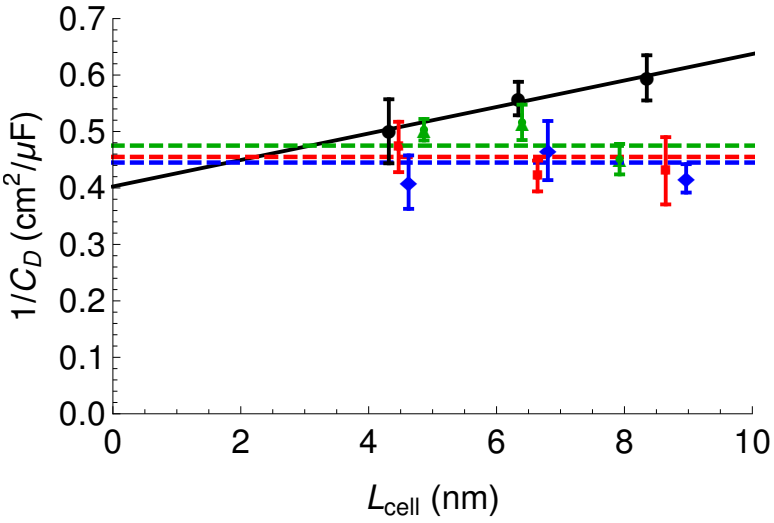

Figure S20: Inverse differential capacitance for dilute 1mol% and 2mol% [$BMIm^+$][BF_4^-] /acetonitrile solutions, pure [$BMIm^+$][BF_4^-] ionic liquid, and neat acetonitrile solvent as a function of the distance between electrodes, L_{cell}. The capacitance is computed for 1/–1 V.

5 Simulations with two graphene layers

Figures S21 and S22 show the results computed for 300 ion pairs of [$BMIm^+$][BF_4^-] when one side of an electrochemical cell is made of two layers of graphene sheets. The differential capacitances in Figure S21 show for all applied voltages, two-layer graphene electrode gives similar differential capacitance to a single layer graphene, and the slight deviation between a single and double layers of graphene electrodes can be attributed to the statistical uncertainties. The charge density profiles in Figure S22 shows that hydrophobic interaction of electrolytes with the two graphene layers is slightly less significant compared to that with a single graphene layer.

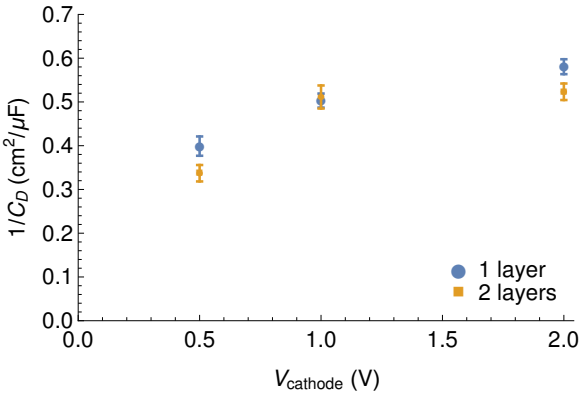

Figure S21: Differential capacitance computed for 300 ion pairs of [BMIm$^+$][BF$_4^-$] when one layer or two layers of graphene is used as an electrode. The applied voltage to cathode/anode are at 0.25/–0.25, 1/–1, and 2/–2 V.

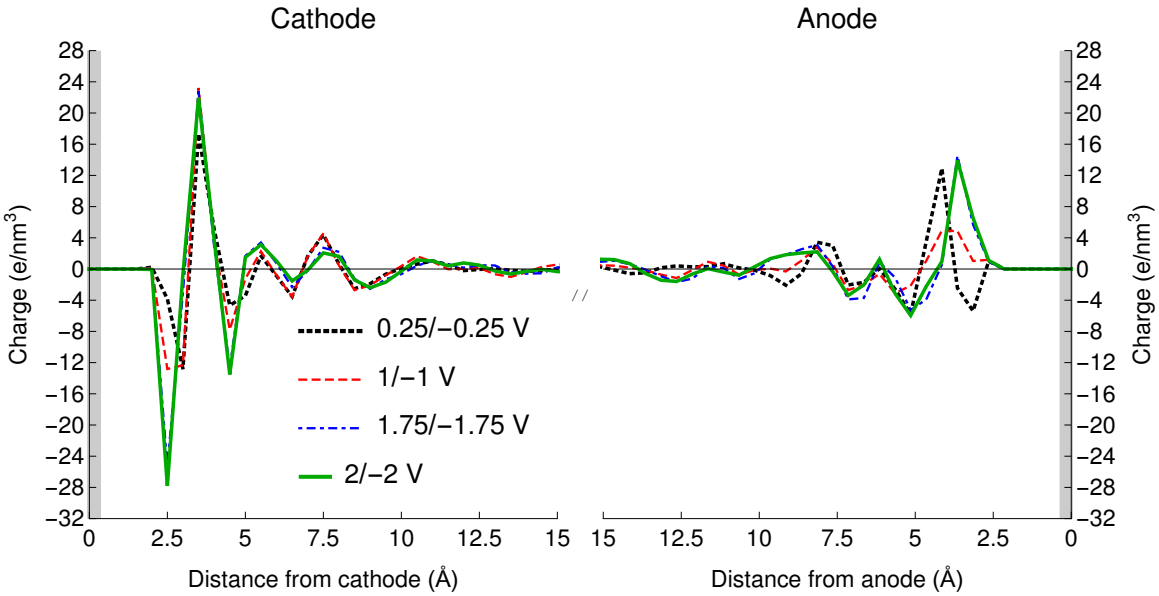

Figure S22: Charge density profiles for 300 ion pairs of [BMIm$^+$][BF$_4^-$] when the applied voltage to cathode/anode (Vcathode/Vanode) are at 0.25/–0.25, 1/–1, 1.75/–1.75, and 2/–2 V. The profiles are calculated when two layers of graphene are used as cathode and anode for simulations.